Basic Science

Surface topography asymmetry maps categorizing external deformity in scoliosis

Amin Komeili, MSc[a], Lindsey M. Westover, MSc[b], Eric C. Parent, PhD, PT[c], Marc Moreau, MD[d], Marwan El-Rich, PhD[e], Samer Adeeb, PhD[f,*]

[a]*Department of Civil and Environmental Engineering, University of Alberta, 5-042 NREF, Edmonton, Alberta T6G 2W2, Canada*
[b]*Department of Mechanical Engineering, University of Alberta, 6-23 MECE, Edmonton, Alberta T6G 2G8, Canada*
[c]*Department of Physical Therapy, University of Alberta, 2-50 Corbett Hall, Edmonton, Alberta T6G2G4, Canada*
[d]*Department of Surgery, University of Alberta, 2C3.77, Edmonton, Alberta T6G 2B7, Canada*
[e]*Department of Civil and Environmental Engineering, University of Alberta, 3-016 NREF, Edmonton, Alberta T6G 2W2, Canada*
[f]*Department of Civil and Environmental Engineering, University of Alberta, 3-025 NREF, Edmonton, Alberta T6G 2W2, Canada*

Received 3 January 2013; revised 28 August 2013; accepted 19 September 2013

Abstract

BACKGROUND CONTEXT: Adolescent idiopathic scoliosis (AIS) affects 2% to 4% of the population and predominantly affects female individuals. The scoliosis researchers and clinical communities use the ''Cobb angle'' obtained from anterior-posterior radiographs as the standard assessment tool for scoliosis. However, excessive radiation exposure over consecutive visits during the growing years increases the risk of cancer in young patients with AIS. Surface topography (ST) is a noninvasive method that is being investigated as an alternative tool for scoliosis assessment. The necessity of applying markers by skilled operators, which is time consuming and a potential area for errors, is one of the main limitations of these methods.

PURPOSE: This study introduces a three-dimensional markerless analysis technique for assessing torso asymmetry in AIS and a system for classifying patients based on this technique. The intra/interobserver and test-retest reliability and validity of the classification system was assessed.

STUDY DESIGN: A novel three-dimensional analysis technique of ST data of patients with scoliosis and its clinical applications.

METHODS: Full-torso ST scans of 46 patients with AIS (Cobb angle: $34 \pm 15°$, curve types: Lenke 1, 3, and 5) and five healthy subjects were used for analysis. The best plane of symmetry, dividing the torso into left and right, was calculated for each scan. The deviation between the original torso and its reflection with respect to the best plane of symmetry was illustrated using deviation contour maps. The subjects were visually classified into three main groups and six subgroups based on the number and location of the asymmetry contours. A second baseline scan and a 1-year follow-up scan were analyzed for 15 subjects and reliability of the method was assessed using kappa coefficients. Funding for this research is provided by the Scoliosis Research Society, Women and Children's Health Research Institute, and the Natural Sciences and Engineering Research Council of Canada.

RESULTS: The intraobserver reliability of the group classification demonstrated excellent agreement with mean kappa coefficient of 0.85. The multiobserver kappa value of 0.62 was attained in the interobserver reliability test conducted among four observers classifying 46 subjects in three groups. The test-retest reliability of the method was assessed. Mean kappa values of 0.99 and 0.83 were achieved for group (three groups) and subgroup (six subgroups) classifications, respectively. The classification system showed good reliability when five observers classified the first baseline and the 1-year follow-up scans.

CONCLUSIONS: A novel method to examine torso asymmetry in patients with AIS is presented, using noninvasive ST scans and a visually intuitive asymmetry map. Distinct patterns of asymmetry

The disclosure key can be found on the Table of Contents and at www.TheSpineJournalOnline.com.

* Corresponding author. Department of Civil and Environmental Engineering, University of Alberta, 3-025 NREF, Edmonton, Alberta T6G 2W2, Canada. Tel.: (1) 780-492-2190.

E-mail address: adeeb@ualberta.ca (S. Adeeb)

were identified allowing patients to be classified into three groups, with six subgroups based on their asymmetry map with very good to excellent reliability. The presented technique shows promise to provide a noninvasive tool for assessment and monitoring of AIS.   © 2014 Elsevier Inc. All rights reserved.

Introduction

Scoliosis is associated with both a lateral deviation and an axial rotation of the spine. Adolescent idiopathic scoliosis (AIS) is the most common form. AIS affects 2% to 4% of the population [1] and predominantly affects female subjects. Typical posture changes resulting from scoliosis include asymmetry in the shoulders, trunk, and scapula and a thoracic prominence.

Most patients do not require treatment unless the curvature progresses [2]. Therefore, frequent observation is required to determine if scoliosis curvatures worsen during the growing years. Radiography is the usual method to assess the severity of scoliosis, monitor progression, and guide treatment decisions. The standard measurement to quantify the scoliosis deformity is the Cobb angle, which is measured on two-dimensional (2D) posterior-anterior radiographs [3]. The Cobb angle is the coronal plane angle measured between the vertebrae at the upper and lower limits of the curve [4]. Increases in Cobb angle of more than 5° suggest progression [5]. Although the Cobb angle technique is the accepted standard, it has several limitations, including suboptimal reliability as well as exposing patients to harmful radiation, which can increase the risk of cancer for the patient population [6,7]. Additionally, radiographic measurements such as the Cobb angle are limited to 2D planar projections, which do not capture the full three-dimensional (3D) nature of the deformity [8]. The lateral deformation and the axial rotation of the spine are biomechanically coupled in scoliosis [8]. Alternative monitoring strategies are needed to reduce radiation exposure and to better quantify the 3D deformity. In addition, radiographs quantify the internal deformity that is only due to scoliosis. However, it is also important to assess the appearance of the torso, which is often more bothersome to patients and has a psychological impact on their quality of life [9].

Surface topography (ST) is a noninvasive assessment of the external torso geometry. ST uses a noncontact optical system to capture the 3D geometry of the torso. The scoliosis deformity can then be quantified by analyzing the torso deformity and the results can complement the x-ray measurements [10–19].

Moiré fringes [20–24], raster-stereography [25], the integrated shape imaging system (Oxford Metrics Ltd., Oxford, UK) [26,27], the Quantec system [28], and the INSPECK system (Creaform Inc., Lévis, QC, Canada) [29] are several ST measurement systems that have been used to digitize patient torsos to create 3D models. A variety of parameters have been proposed to quantify the 3D torso deformity. Most parameters are based on distances and angles between landmarks identified on the torso [30,31], or on geometric properties of 2D cross sections through the torso [13]. One such parameter aims to quantify the left-right asymmetry of the back surface based on reflecting a set of three index points across the medial sagittal plane [32]. This is based on the assumption that the median sagittal plane is a plane of symmetry for the back surface. However, for a patient with AIS, this plane does not necessarily represent the best plane of the symmetry due to the axial and lateral rotations of the spine.

In this study, we introduce a novel symmetry analysis technique that uses the full 3D ST data without the need for markers. The proposed technique overcomes the limitations associated with marker placement. Because the markers are manually placed, it is difficult to consistently place them in the appropriate anatomical locations. This new technique is based on identifying the best sagittal plane of symmetry and allows visualization of the extent of asymmetry on the whole torso rather than using 2D measures that would be limited to specific areas or distances.

Spinal deformities associated with scoliosis can be classified into different curve types. Classification systems may be useful in estimating prognosis and guiding treatment decisions. Such systems also may be useful in constructing measures of severity that are specific to a certain category or type of deformation. The Lenke [33] classification system is commonly used to classify curve patterns based on the shape and location of the deformity within the spine. Three radiographs are used to classify the spinal deformities in a Lenke type. However, the Lenke classification was developed only to plan surgeries [33] and does not account for the external deformities or the esthetic appearance of the patient. To our knowledge, there are no classification systems for scoliosis based on symmetry analysis of the torso surface.

In this article, we present a classification system based on the torso deformity measured from the ST data. The proposed system will allow classification of the torso deformity into different groups such that for each group the torso deformity and curve progression can be measured and assessed separately. In addition, the classification system has the potential to allow better correlations between the external torso surface and the internal deformity.

The objectives of this study were (1) to develop a novel analysis technique to classify the torso asymmetry for

patients with AIS based on noninvasive ST assessment, (2) to develop a classification system for patients with scoliosis into categories based on asymmetry maps created in objective 1 and to determine the reliability of the proposed classification system, (3) to determine whether patients change torso asymmetry classification when analyzing ST scans taken 1 year apart for the same patient, and (4) to compare the pattern of the asymmetry map with the shape of the spine in corresponding radiographs.

Materials and methods

Subjects

Full-torso ST scans were retrieved from an ongoing study for 50 patients with AIS from the Edmonton Scoliosis Clinic database and five healthy subjects. The mean Cobb angle was 34.1° (minimum 12°, maximum 67°). There were 13, 10, and 23 subjects with Lenke 1, Lenke 3, and Lenke 5 curve types, respectively. Four subjects with AIS were excluded because of poor reconstruction or noise in the data; thus, 46 subjects with AIS were used for the analysis. For the same-day test-rest analysis, a second scan was acquired a few minutes after the first scan and was used for assessing the reliability in 15 randomly selected subjects. Patients stepped out of the positioning frame and were repositioned between scans. For objective 2, an additional scan captured 1 year later was analyzed for these same 15 randomly selected subjects, among which 7 patients had been treated with braces and 8 did not receive treatment. The mean Cobb angle at the 1-year follow-up was 32.7° (minimum 14°, maximum 92°). All patients selected were diagnosed with AIS, had no surgical treatment, and were between 10 and 18 years old. Healthy volunteer participants were selected if they had no diagnosis of spinal deformity, scoliometer measurements inferior to 7°, complete pain-free range-of-motion (ROM) of the spine, and pain-free ROM of the lower extremities. Approval from the human research ethics board was obtained and subjects provided informed consent.

Data acquisition

Data were collected as described previously [34,35] using four VIVID 910 3D laser scanners (Konica Minolta Sensing Inc., Ramsey, NJ, USA) placed in the corners of a square room and distanced 3 m from each other. The subjects stood in a frame to standardize the position of the subjects relative to the scanners (Fig. 1). The position of the feet was standardized to shoulder width on a platform. The shins were aligned in the frontal plane by positioning the patient such that both shins touched a horizontal bar just below the knee. The arms were positioned at 90 degrees of elevation by adjustable supports placed under the elbows. A probe placed just above C7 offers feedback to the subjects to limit the postural sway from their natural standing position. The accuracy of each scanner with the WIDE lens is
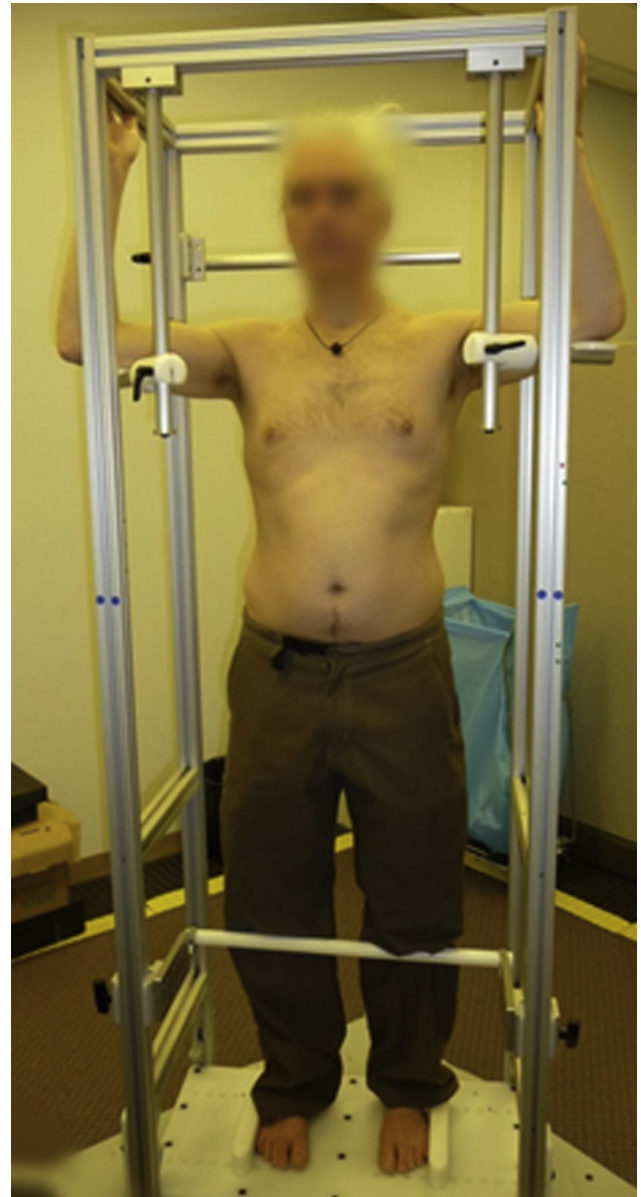

Fig. 1. Supported position of the patient in the frame.

±1.4, ±0.4, and ±0.4 mm along the depth, width, and height axes, respectively.

Data preprocessing

The four views from the cameras were merged together using the Polygon Editing Tool (PET version 2.21, Konica Minolta) to create a model of each subject's full torso. The data were exported as a point cloud and imported into the Geomagic software (Geomagic Studio 12, Morrisville, NC, USA). The points representing the frame, arms, hips, head, and neck were manually selected and deleted. The lower portion of the torso was cropped at the pants line. Pants were always pulled down below the posterior superior iliac spine during scanning. The subject's head was
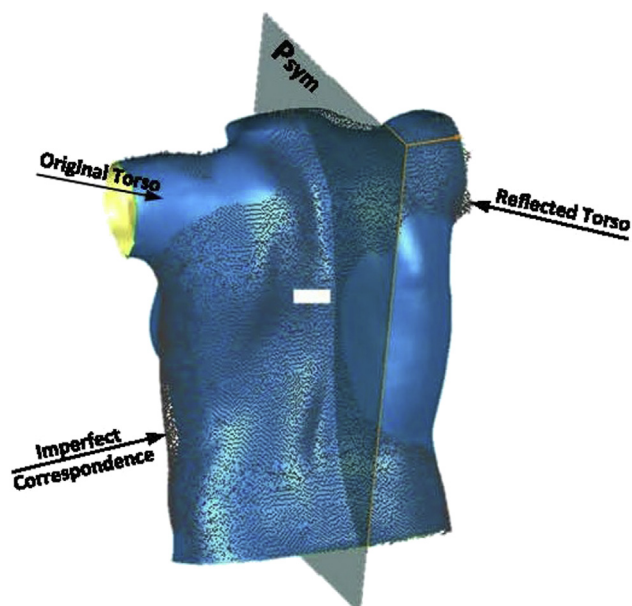
Fig. 2. Solid surface and cloud of points representing the original and reflected torsos, respectively, along with the best plane of symmetry (Psym).

obtained. This ''Psym'' is the plane that minimizes the distance between the original torso and its reflection. Then, the cloud of points of the scanned torso (the ''original torso'') was reflected to create a ''reflected torso.'' Figure 2 shows the overlaying of the cloud of points of the reflected torso on top of the triangulated surface of the original torso, as well as the best plane of symmetry. In the second step, a color map of the deviation between the original and the reflected torso was drawn that clearly shows the areas affected by the scoliosis deformity. The green color indicates a deviation of -3 to 3 mm between the original and the reflected torso. Blue colors indicate that the original torso is bulging out compared with the reflected torso and red colors indicate that the original torso is inside of the reflected torso. A left-right pair of corresponding blue and red colors in the asymmetry map is termed a color patch (Fig. 3). For example, a rib hump on the right side of a patient would be characterized by a blue color deviation on the right side (because the original torso would be outside the reflected one) and a corresponding red color deviation on the left side. The technical details of the implementation of the two steps are described in the Supplementary Appendix.

Classification into external deformity groups

The back and front views of the asymmetry map for each subject's torso were visually appraised by three scoliosis professionals (AK, LW, SA), to identify possible categories for the surface classification. Categories were identified based on the number and location of the asymmetry contours present in the asymmetry maps.

Reliability

The intraobserver, interobserver, and test-retest reliability of classifying subjects with AIS into the proposed categories was evaluated. Eight observers were asked to classify patients based on the asymmetry maps. Three

cropped at approximately the level of the shoulders. The arms were cut through the corners of the acromion.

For several patients, some surfaces were not properly captured by the cameras, such as the top of the shoulders and the lateral side of waist. These zones created holes and spikes in the torso models. Additionally, the models had areas of overlapping points due to the merging process. To obtain a smooth cloud of points representing the torso geometry, the Geomagic built-in functions ''Fill Single'' were used to fill in the small holes and to correct these scanning artifacts.

Asymmetry analysis

The asymmetry analysis consisted of two steps. In the first step, the ''best plane of symmetry (Psym)'' was
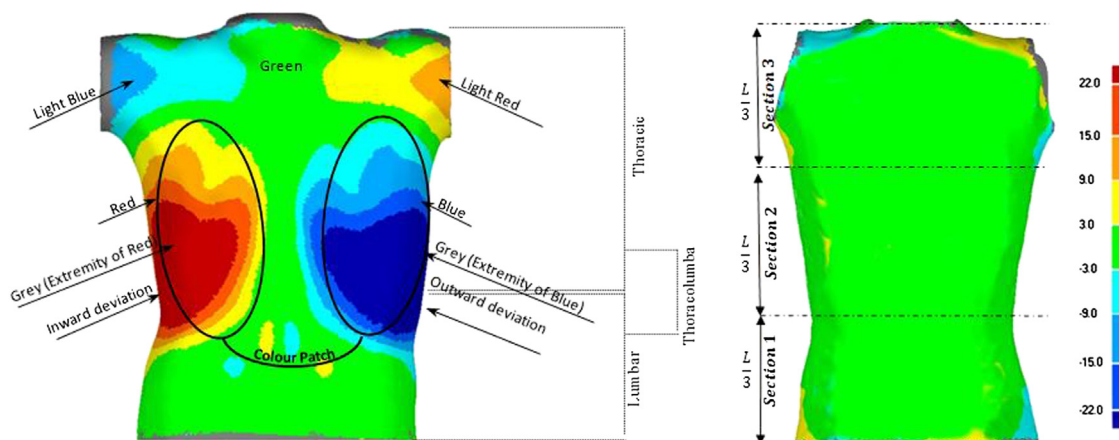

Fig. 3. Analyzed torso models and contour maps for (Left) subjects with scoliosis and (Right) healthy subjects.

Table 1
The Lenke curve type, Cobb angle (degrees), and treatment of 15 patients with 1-year follow-up data

ID	Lenke type	Baseline curve	Follow-up curve	Treatment
1	1	26R MT; 18L TL/L	22R MT; 13L TL/L	Observation
2	1	67R MT	92R MT	Observation
3	1	18L PT; 27R MT	18L PT; 17R MT	Brace
4	3	46L PT; 59R MT; 34L TL/L	46L PT; 58R MT; 37L TL/L	Brace
5	5	15L TL/L	18L TL/L	Observation
6	5	14L TL/L	14L TL/L	Observation
7	5	44L TL/L	48L TL/L	Observation
8	5	26L TL/L	25L TL/L	Observation
9	5	33R TL/L	30R TL/L	Observation
10	5	22R MT; 35L TL/L	20R MT; 34L TL/L	Observation
11	5	25R TL/L	28R TL/L	Brace
12	5	25L TL/L	23L TL/L	Brace
13	5	21R MT; 38L TL/L	18R MT; 34L TL/L	Brace
14	5	12L TL/L	15L TL/L	Brace
15	5	32L TL/L	32L TL/L	Brace

L, left; MT, main thoracic; PT, proximal thoracic; R, right; TL/L, thoracolumbar/L.

observers were experienced scoliosis researchers, whereas the remaining five did not have specific knowledge about scoliosis. The ability to distinguish the colors was the only qualification criterion for the observers. The classification system was summarized in a two-page instruction manual to ensure that the definitions of the classification system and procedure of categorization were understood by all observers. The first author explained the content of the instruction manual to the observers before performing the test.

The reliability was measured by the kappa coefficient, which determines the extent of agreement between repeated assignments of subjects to nominal categories [36]. Poor, fair, moderate, good, and excellent agreements are indicated by the ranges 0 to 0.20, 0.21 to 0.40, 0.41 to 0.60, 0.61 to 0.80, and 0.81 to 1.00, respectively [36].

Intraobserver reliability

To determine intraobserver reliability, four observers classified the group of 46 subjects with AIS two times, leaving at least 3 days between each trial to minimize memory bias. The kappa coefficient and the percentage of agreement ($P_0\%$) between the two trials were determined for each observer. The reliability was reported as the average of the four calculated kappa coefficients and the four calculated $P_0\%$ values.

Interobserver reliability

To determine interobserver reliability, four observers classified the group of 46 subjects with AIS. The multiobserver kappa coefficient and the $P_0\%$ were determined.

Intraobserver test-retest reliability

The second baseline scan of the 15 selected patients was compared with the first scan to assess the test-retest reliability of the classification. This analysis includes the error due to the effect of patient posture and model preparation. The 15 pairs of torso models were randomized and five observers were asked to classify the 30 models. The intraobserver test-retest kappa coefficient and the $P_0\%$ between the two scans were determined for each observer. The reliability was reported as the average of the five calculated kappa coefficients and the five calculated $P_0\%$ values.

One-year follow-up test-retest reliability

The follow-up ST scan was acquired approximately 1 year after the baseline scans and analyzed for 15 selected subjects. Table 1 shows the Lenke curve type, Cobb angles at baseline and 1 year, and the treatment received during the 1-year interval for each subject. The mean curve progression for these patients was 4° (minimum −10°, maximum 25°) with standard deviation (SD) of 6.04° and none of the patients changed Lenke curve type during the 1-year interval. Subjects were not selected on the basis of whether or not they had progressed during the follow-up to reflect the likelihood that classification would change in the population seen longitudinally at our clinic. Because the Lenke curve types did not change over the 1-year span, the pattern of torso asymmetry was expected to stay the same as well. The 30 models from the 15 pairs of torso models (first baseline and 1-year follow-up) were randomized and five observers were asked to classify each asymmetry map. The kappa coefficient and the $P_0\%$ for the classification based on baseline and 1-year scans were determined for each observer. The 1-year test-

Table 2
Intraobserver reliability of torso classification by the four observers

Observers	Group classification				Subgroup classification			
	$P_0\%$	κ	95% CI	Strength of agreement	$P_0\%$	κ	95% CI	Strength of agreement
1*	96	0.92	0.81–100	Excellent	80	0.75	0.61–0.90	Good
2	91	0.84	0.69–0.99	Excellent	83	0.78	0.65–0.92	Good
3	83	0.68	0.48–0.87	Good	78	0.72	0.57–0.87	Good
4	93	0.88	0.74–1.00	Excellent	76	0.70	0.55–0.85	Good
Average	91	0.85		Excellent	79	0.74		Good

CI, confidence interval; $P_0\%$, percentage of agreement.
* Scoliosis professional observer.

Table 3
Distribution of classification decisions by each pair of observers from the sample of four observers when rating 46 subjects into three groups

	Group A	Group B	Group C	Total
Group A	137			137
Group B	39	70		109
Group C	8	10	12	30
Total	184	80	12	276

retest reliability was reported as the average of the five calculated kappa coefficients and the five calculated $P_0\%$ values to reflect the stability of the classification over a 1-year interval.

Comparison with x-rays

The correspondence between the shape of the spine on radiograph and the pattern of the asymmetry map from the ST analysis was examined for each of the 46 subjects at baseline. The x-ray picture was aligned, scaled, and overlapped on the asymmetry map. Alignment was done by matching the neck and shoulder lines that are visible in both the x-ray and the ST asymmetry map. Scaling was achieved by using the scale on the radiograph and adjusting the image so that 1 cm measured on the radiograph corresponded to 1 cm in the geometric model of the torso surface.

Results

Asymmetry analysis

Asymmetry analysis was completed on 51 of the original 55 subjects (46 subjects with AIS and 5 healthy subjects). Figure 3 shows an example of the asymmetry map obtained from the analysis for an AIS and a healthy subject.

Three broad classification groups subdivided into a total of six subgroups were identified among the asymmetry maps (Supplementary Table). The three groups (Groups A, B, and C) were identified based on the number of color patches on the torso. The reader is reminded that a pair of corresponding blue and red colors in the asymmetry map is termed a color patch (section 2.4). The location of each color patch is described in reference to the bottom third (section 1), middle third (section 2), or top third (section 3) of the torso (Fig. 3). A schematic and a description of each group and its subgroups are shown in the Supplementary

Table. Group A contains three subgroups, each having two color patches along the torso height. In subgroups A1 and A2, the center of the largest color patch is located in the thoracic or thoracolumbar region, whereas it is in the lumbar region in subgroup A3. Subgroup A2 has asymmetry extending to the scapula, whereas subgroup A1 does not. Group B, with its subgroups B1 and B2, is characterized by having three color patches along the height of the torso with the center of the largest color patch located in thoracolumbar or lumbar regions. Subgroup B2 has asymmetry in the scapula area, whereas subgroup B1 does not. Group C, which includes subgroup C1, has four color patches through the torso height.

As described in the "Data preprocessing" section, the asymmetry analysis determines the distance from each point in the original torso to its corresponding point in the reflected torso, and displays these distances in the form of a color map (asymmetry map). The SD of these distances is also calculated for each analysis. The SD values for the subjects with AIS classified into Group A, Group B, and Group C were 7.6±3.1 mm, 8.3±2.8 mm, and 6.5±3.5 mm, respectively. The SD for the five healthy subjects was 3.4±0.8 mm.

Reliability

Intraobserver reliability

The average kappa coefficient for the intraobserver reliability of those who classified the 46 subjects into the three broad groups was 0.85 (range 0.68 to 0.92), indicating good to excellent reliability (Table 2). When considering the six subgroups, the kappa coefficient showed good intraobserver reliability (average 0.74, range 0.70–0.78), indicating that the observers are able to consistently classify the subjects into the same category (Table 2).

Interobserver reliability

Good interobserver reliability was found among the four observers in classifying into both the three groups and the six subgroups. For the three-group classification, the multi-observer kappa value was 0.62 and the percentage of agreement was 80%, indicating moderate reliability. For classification into the six subgroups, the corresponding values were 0.52% and 59%, respectively, indicating moderate reliability.

Table 4
Distribution of classification decisions by each pair of observers from the sample of four observers when rating 46 subjects into six subgroups

	Subgroup A1	Subgroup A2	Subgroup A3	Subgroup B1	Subgroup B2	Subgroup C1	Total
Subgroup A1	33						33
Subgroup A2	22	62					84
Subgroup A3	7	3	10				20
Subgroup B1	7	5	9	37			58
Subgroup B2	4	9	5	16	17		51
Subgroup C1	2	2	4	6	4	12	30
Total	75	81	28	59	21	12	276

Table 5
Test-retest reliability: comparing the classification of the first and second baseline scans of 15 torsos

Observers	Group classification				Subgroup classification			
	$P_0\%$	κ	95% CI	Strength of agreement	$P_0\%$	κ	95% CI	Strength of agreement
1*	100	1	1.00–1.00	Excellent	93	0.91	0.74–1.00	Excellent
2	87	0.62	0.15–1.00	Good	80	0.70	0.41–0.99	Good
3	80	0.32	−0.28 to 0.92	Fair	80	0.73	0.48–0.98	Good
4*	93	0.89	0.67–1.00	Excellent	80	0.75	0.51–1.00	Good
5*	100	1	1.00–1.00	Excellent	93	0.92	0.76–1.00	Excellent
Average	92	0.99		Excellent	85	0.83		Excellent

CI, confidence interval; $P_0\%$, percentage of agreement.
* Scoliosis professional observers.

To assess the discrepancy in classification between observers, the frequency of their classification can be shown in matrix format. The classifications by each pair of observers for the 46 subjects were compared (six comparisons in total for four observers) and are summarized in Table 3 for groups and Table 4 for subgroups. The diagonal components of the matrix indicate the number of times two observers agreed on the classification for a particular subject. The off-diagonal components indicate when two observers disagreed on the classification for a particular subject, and the location of the entry in the matrix indicates which categories were selected in each disagreement. For example, in Table 3, there were 39 instances when one observer classified a subject into Group A and another observer classified the same subject into Group B.

Intraobserver test-retest reliability

Figure 4 shows typical asymmetry maps of the first and second baseline scans of a patient. The average percent difference in SD value between the first and second baseline scan among the 15 analyzed subjects was 14% (minimum 1% and maximum 58%) and the asymmetry maps showed similar patterns between the two scans for all patients. The intraobserver test-retest reliability in subgroup classification using the first and second baseline scans of 15 torsos was 85% agreement (range 80%–93%), with a mean kappa value of 0.83 (range 0.70–0.92), indicating good to excellent reliability (Table 5). For the group classification, the percent agreement increased to 92% (range 80%–100%), with a mean kappa value of 0.99 (range 0.32–1.00),

demonstrating that most of the torsos were classified in the same category using the first and second baseline scans. Moreover, the high value of $P_0\%$ and the small difference in the SD (14%) between the first and second baseline scans confirms the repeatability of the method.

One-year follow-up test-retest reliability

Table 6 shows the intraobserver test-retest reliability results of the classification based on the first baseline and 1-year follow-up scans. The mean kappa value of group and subgroup classifications were 0.70 (range 0.56–0.84) and 0.71 (range 0.29–0.82), respectively. Figure 5 shows the asymmetry map of a subject for each of the two scans within a 1-year interval.

Comparison with x-rays

The asymmetry map from the first baseline scan and the corresponding x-ray were examined for all subjects. Examples of this comparison for two patients with mild and severe scoliosis are shown in Fig. 6 along with the asymmetry map for a healthy subject. The torsos of the healthy subjects showed little to no deviation in their asymmetry maps (Fig. 6, Left). It can be observed that the more symmetric the torso, as indicated by the asymmetry map, the straighter the underlying spine is based on the radiograph. Moreover, the location of the apex of the curve on the radiograph is in good agreement with the location of the maximal external deviation. This correspondence is even visible in the subjects with mild scoliosis (eg, Fig. 6, Middle). The correspondence shown in Fig. 6

Table 6
Reliability result of classifying the first and 1-year follow-up scan of 15 torsos

Observers	Group classification				Subgroup classification			
	$P_0\%$	κ	95% CI	Strength of agreement	$P_0\%$	κ	95% CI	Strength of agreement
1*	80	0.56	0.22–0.90	Moderate	80	0.74	0.48–0.99	Good
2	93	0.62	0.15–1.00	Good	87	0.81	0.56–1.00	Excellent
3	93	0.77	0.35–1.00	Good	87	0.82	0.61–1.00	Excellent
4*	80	0.63	0.24–1.00	Good	40	0.29	0.00–0.58	Fair
5*	93	0.84	0.55–1.00	Excellent	73	0.66	0.39–0.93	Good
Average	88	0.70		Good	77	0.71		Good

CI, confidence interval; $P_0\%$, percentage of agreement.
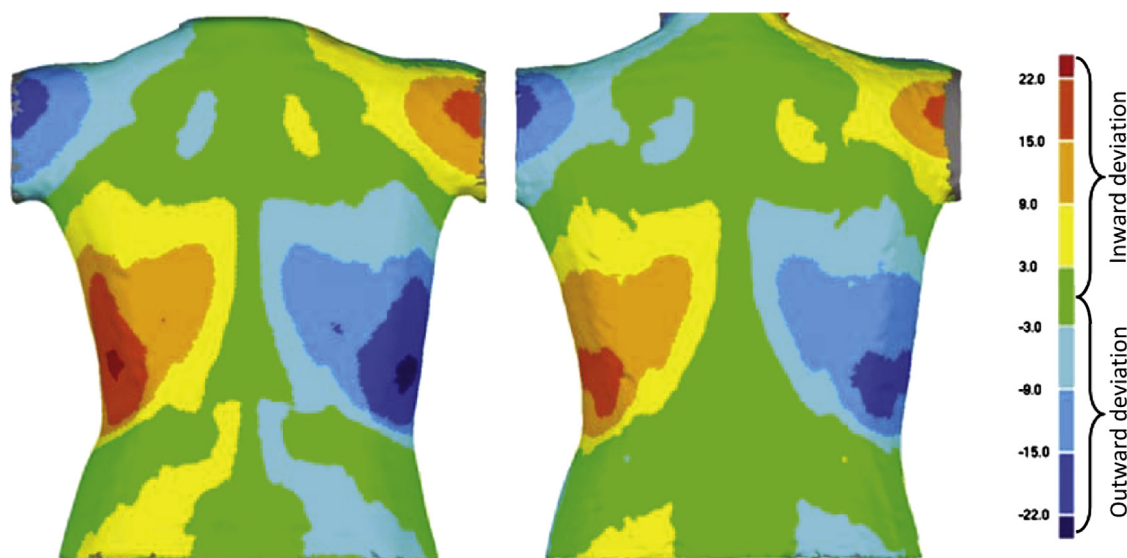* Scoliosis professional observers.

Fig. 4. First (Left) and second (Right) baseline scan for a typical torso (Cobb angle 31R T).

between the radiographs and the ST asymmetry maps was observed for all subjects.

Discussion

In this study, a novel technique was presented to quantify, visually report, and classify torso asymmetry in patients with AIS based on ST data. The proposed method is noninvasive, does not rely on any markers placed on the torso, and uses the full 3D torso data. Three distinct groups divisible into six subgroups with different torso asymmetry patterns were identified based on visual comparison of the asymmetry maps of the analyzed torsos. The intra- and interobserver, short- and long-term test-rest reliability of the

classification indicates that the method is repeatable. However, like other classification systems [37], categorizing some subjects who have characteristics on the boundary between different groups may become complex.

The classification presented here is based on the patterns identified in the asymmetry maps derived from ST data, whereas the Lenke classification system is based on radiographic measures of the spine. Because of this, there is not a direct correspondence between each subgroup in our classification system and one Lenke curve type. For example, subgroups A1 and A2 contain a large color patch in either the thoracic or thoracolumbar region. These patterns would likely correspond to patients who have a curve type of either Lenke 1 or Lenke 5. At the same time, subgroup A3
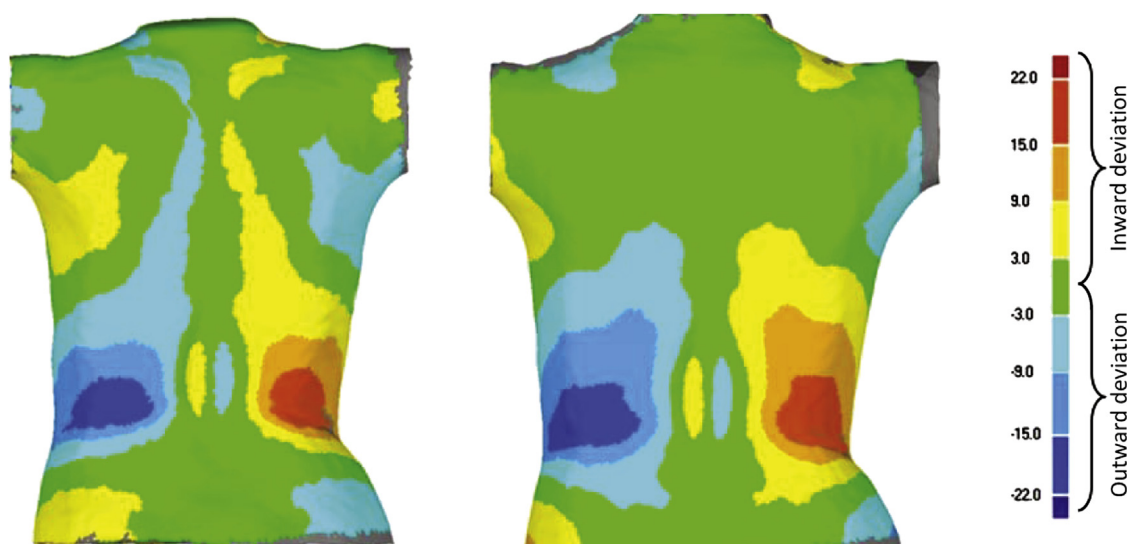

Fig. 5. First scan (Cobb angle 21 right thoracic [R T]; 38 left thoracolumbar [L TL]) (Left) and 1-year follow-up scan (Cobb angle 18R T; 34L TL) (Right) of the selected subject.
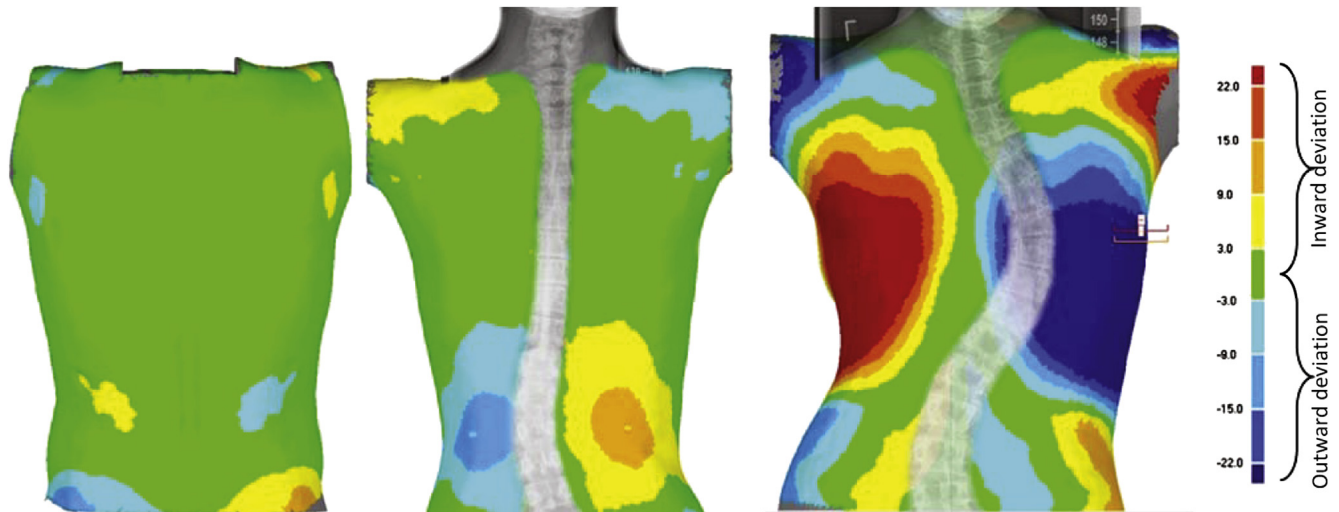
Fig. 6. The surface topography color asymmetry deviation map of subjects with (Left) normal spine, (Middle) mild scoliosis, and (Right) severe scoliosis with their corresponding radiograph. To minimize radiation exposure, the radiograph of the healthy subject was not available.

contains a large color patch in the lumbar region, which may also correspond to patients with a Lenke 5 curve type. The correspondence between the asymmetry classification subgroups and the Lenke curve types was not directly investigated in this study; however, the basis of the two classification systems would suggest that there is not a direct one-to-one correspondence between them.

In our study, we looked only at Lenke types 1, 3, and 5, as our database of ST patients contains too few patients with other Lenke types to allow an analysis with sufficient representation of these groups. However, our analysis technique should work as well for Lenke types 2, 4, and 6, and this will be examined in the future. Lenke 2 consists of a structural curve on the upper thoracic section and thus can hypothetically be identified with subgroups A1 and A2. Similarly, Lenke 4 can be identified with subgroup C1. Lenke 6, which represents a double curve, also can be hypothetically identified with subgroups B1 and B2. Our future studies will look at including other Lenke types in our sample size. Although we expected our classification system to produce excellent reliability results, we realized that there are sources of discrepancies during the process of visual categorization. The most common difficulties encountered by the observers included the distinction of subgroup A1 from subgroup B1 and subgroup A2 from subgroup B2. These discrepancies occurred when one or more small patches of asymmetry were ignored in section 1 (Fig. 3, Right) in some trials (or by some observers) and counted in others. Another difficulty was identifying the difference between subgroups A1 and A2 and subgroups B1 and B2 when the extended deviation on the shoulder/scapula region was ignored by some observers and counted by others. However, the mean kappa value of 0.85 (range 0.68–0.92) obtained for intraobserver reliability and multiobserver kappa coefficient of 0.62 calculated for

interobserver reliability demonstrates comparable reliability with respect to the Lenke classification system [33]. In their study, five surgeons who had developed the Lenke classification system used both the Lenke and the King classification for a group of patients. Kappa values of 0.83 (range 0.79–1.00) and 0.92 (range 0.83–1.00) were reported for the intraobserver and interobserver reliability of classifying the curve type, respectively using the Lenke classification and 0.62 and 0.49 using the King classification [37]. However, no multiobserver kappa was reported in Lenke et al.'s study [33]. The reliability of the present system may possibly be improved by clarifying the manual for the proposed classification system with precise values of deviation for the different categories or providing more observer training.

Selecting an appropriate spectrum for the color map of the deviation analysis assists the observer in distinguishing the category. Using a large number of colors would make the torso a compound of colors that might distract the observers, whereas a reduced number of colors might conceal some features of the torso deformity. Likewise, a wide range of maximum and minimum deviation would not reveal the mild deformity, whereas a narrow range would not illustrate the variations among the severely asymmetric torsos. Our proposed spectrum, with nine colors and a maximum deviation of ±22 mm, was selected after trying a variety of different settings for the full set of torsos models. Our chosen spectrum allows categorizing all curves encountered in this study.

The $P_0\%$ for the group classification (92%) and the subgroup classification (85%) shows that the pattern of torso deformity was nearly the same in the first and second baseline scans for the examined subjects. This suggests that positioning the patient during the scan and preprocessing the torso geometry for analysis were reproducible and do not

significantly affect the classification based on the asymmetry analysis of the torso. This suggests that our classification system is repeatable and provides a method to group patients according to their ST asymmetry map irrespective of the time at which the data were acquired.

In every case, the P_0% for the group classification was greater than or equal to the corresponding value for the subgroup classification. In general, this is because it is more difficult to classify the subjects into six groups than three. With six subgroups, chance agreement is also less likely than with three groups. With the six subgroups, the boundaries between the subgroups are more subtle, and some asymmetry maps may lie on these boundaries. It can be seen from Table 3 that the number of agreements between observers for the three-group classification, represented by the diagonal entries, is generally high when compared with the number of disagreements. However, in Table 4, the large values in the A1, A2 and B1, B2 entries indicate areas of uncertainty among the observers in distinguishing subgroup A1 from A2 and subgroup B1 from B2.

The 1-year interval test-retest reliability coefficients and visual comparison of the asymmetry maps between the baseline and 1-year follow-up in patients for which Lenke curve types had not changed during the interval showed that ST asymmetry group classification is reliable. Classification decisions remained the same for most of the 15 patients analyzed throughout the 1-year time interval. Even if the magnitude or severity of the deformity changed between the baseline and 1-year follow-up scans, the asymmetry deviation contour map and classification were found to be the same. Observer 4 was found to have good reliability in the group classification for this analysis, but only fair reliability in the subgroup classification (kappa 0.29). This lower reliability may be because of the difficulties distinguishing the different subgroup categories, as discussed previously. However, it may also be because of differences in the torso asymmetry map from treatment or progression of the scoliosis deformity. It was found that 40% of the discrepancies in subgroup classifications for observer 4 were related to subjects with a change in Cobb angle of more than 4° (subject ID 2, 3, 11, and 13 in Table 1).

Although our classification system was found to be reliable, it is not meant as a quantitative measure of asymmetry. The SD of the deviation over the full torso summarizes the severity of the asymmetry; however, it does not quantify the extent of asymmetry in specific regions (ie, areas of high asymmetry). This measure, however, shows a promise in distinguishing between patients with scoliosis and healthy patients. For patients with scoliosis, we obtained SD values of 7.6±3.1 mm, 8.3±2.8 mm, and 6.5±3.5 mm for groups 1, 2, and 3, respectively. These values are almost twice the magnitudes for healthy subjects (3.4±0.8 mm). Future work will focus on augmenting our qualitative classification system with measures that are dependent on SD in hopes that these measures can objectively assess the severity of the deformity most appropriately within each category. Although the classification system was found to be reliable, the validity, reliability, and sensitivity to change of the suggested parameters should be assessed in the future. In addition, the comparison between the deformities measured using the x-ray and the obtained asymmetry map will be further investigated to determine the relationship between the external deformity and the internal spinal geometry.

Classifying the torsos based on the asymmetry map derived from ST scans has the potential to noninvasively detect torso asymmetry associated with scoliosis. Further, this classification may assist with monitoring progression noninvasively if parameters can be extracted reflecting progression with high sensitivity to change in each classification category. We believe that the asymmetry analysis and associated classification system have the potential to assist with monitoring progression; the proposed system is able to draw the attention of the clinicians to areas of change and consequently may reduce the number of x-rays required for patient follow-up. Further, classification of surface deformities may guide the design of personalized braces by identifying areas of the surface most affected by scoliosis. Bracing uses surface pressures to correct the effect of scoliosis and to prevent further progression. Therefore, the proposed classification may help direct these therapies to address the most asymmetric features for the patients.

The success in classifying the torso based on markerless ST data may lead to the development of severity measures that are specific to each group, which might overcome the limitations of the current ST measures. For example, in the current ST measures, the parameters of measurement are not specific to a certain curve type, so changes in some patients captured by a change in some severity indicators are diluted when averaged with the same measurements obtained from patients with a different curve type.

Conclusion

In this article, we were able use a simple geometric approach to create deviation color maps between the torso and its reflection from which the scoliosis deformities can be visualized. Our approach does not rely on any markers and thus avoids the inherent errors associated with placing landmarks on the patients and digitizing landmarks during the analysis. The created deviation color maps followed certain patterns that allowed the creation of a reliable classification system based on ST. The deviation color maps exhibited a correspondence with the underlying spine as visualized in the patient's x-ray. In addition, it was observed that a patient's individual group (color pattern of the deviation maps) did not change over time among the 15 subjects with a 1-year follow-up. We hope that our categorization method will allow the development of ST measures specific to subgroups of patients with similar scoliosis deformities.

Appendix

Supplementary material

To access the supplementary materials, please visit the online version of *The Spine Journal* at http://dx.doi.org/10.1016/j.spinee.2013.09.032.

References

[1] Rogala EJ, Drummond DS, Gurr J. Scoliosis: incidence and natural history. A prospective epidemiological study. J Bone Joint Surg 1978;60:173–6.

[2] Asher MA, Burton DC. Adolescent idiopathic scoliosis: natural history and long term treatment effects. Scoliosis 2006;1:2.

[3] Reamy BV, Slakey JB. Adolescent idiopathic scoliosis: review and current concepts. Am Fam Physician 2001;64:111–6.

[4] Cobb RJ. Outline for study of scoliosis, American Academy of Orthopaedic Surgeons, instructional course lectures. St Louis, MO: CV Mosby, 1948:261–75.

[5] Richard BS, Bernstein RM, D'Amato CR, Thompson GH. Standardization of criteria for adolescent idiopathic scoliosis brace studies: SRS committee on bracing and nonoperative management. Spine 2005;30:2068–75.

[6] Viviani GR, Budgell L, Dok C, Tugwell P. Assessment of accuracy of the scoliosis school screening examination. Am J Public Health 1984;74:497–8.

[7] Levy AR, Goldberg MS, Mayo NE, et al. Reducing the lifetime risk of cancer from spinal radiographs among people with adolescent idiopathic scoliosis. Spine 1996;21:1540–8.

[8] Thulbourne T, Gillespie R. The rib hump in idiopathic scoliosis: measurement, analysis and response to treatment. J Bone Joint Surg Br 1976;58:64–71.

[9] Lai SM, Asher M, Burton D. Estimating SRS-22 quality of life measures with SF-36: application in idiopathic scoliosis. Spine 2006;31:473–8.

[10] Stokes IAF, Moreland MS. Concordance of back surface asymmetry and spine shape in idiopathic scoliosis. Spine 1989;14:73–8.

[11] Poncet P, Delorme S, Ronsky JL, et al. Reconstruction of laser-scanned 3D torso topography and stereoradiographical spine and rib-cage geometry in scoliosis. Comput Methods Biomech Biomed Engin 2000;4:59–75.

[12] Goldberg CJ, Kaliszer M, Moore DP, et al. Surface topography, Cobb angles and cosmetic change in scoliosis. Spine 2001;26:E55–63.

[13] Jaremko JL, Poncet P, Ronsky J, et al. Genetic algorithm-neural network estimation of Cobb angle from torso asymmetry in scoliosis. J Biomech Eng 2002;124:496–503.

[14] Mohsen MES. Comparison of roentgenography and Moiré topography for quantifying spinal curvature. Phys Ther 1986;66:1078–82.

[15] Montgomery F, Persson U, Benoni G, et al. Screening for scoliosis: a cost effectiveness analysis. Spine 1990;15:67–70.

[16] Nissinen M, Heliovaara M, Ylikoski M, Poussa M. Trunk asymmetry and screening for scoliosis: a longitudinal cohort study of pubertal schoolchildren. Acta Paediatr 1993;82:77–82.

[17] Pearsall D, Reid JG, Hedden DM. Comparison of three noninvasive methods for measuring scoliosis. Phys Ther 1992;72:648–57.

[18] Pruijs JEH, Keessen W, van der Meer R, et al. School screening for scoliosis: methodologic considerations. Spine 1992;17:431–6.

[19] Sakka SA, Wojcik A, Macindoe S, Mehta MH. Three-dimensional analysis of spinal deformity. Stanmore, England: IOS Press, 1995:111–5.

[20] Daruwalla JS, Balasubramaniam P. Moiré topography in scoliosis: its accuracy in identifying the site and size of the curve. J Bone Joint Surg Br 1985;67:211–3.

[21] Laulund T, Sojbjerg JO, Horlyck EH. Moiré topography in school screening for structural scoliosis. Acta Orthop Scand 1982;53:765–8.

[22] Sahlstrand T. The clinical value of Moiré topography in the management of scoliosis. Spine 1986;11:409–17.

[23] Moreland MS, Pope MH, Wilder DG, et al. Moire fringe topography of the human body. Med Instrum 1981;15:129–32.

[24] Suzuki N, Armstrong GWD, Armstrong J. Application of Moiré topography to spinal deformity. In: Moreland MS, Pope MH, Armstrong GWD, eds. Moiré fringe topography and spinal deformity. Oxford, UK: Pergamon Press, 1981:225–40.

[25] Hierholzer E, Frobin W. Rasterstereography measurement and curvature analysis of the body surface of patients with spinal deformities. In: Moreland MS, Pope MH, Armstrong GWD, eds. Moiré fringe topography and spinal deformity. Oxford, UK: Pergamon Press, 1981:267–76.

[26] Theologis TN, Jefferson RJ, Simpson AH, et al. Quantifying the cosmetic defect of adolescent idiopathic scoliosis. Spine 1988;18:909–12.

[27] Turner-Smith AR, Harris JD, Hougton GR, Jefferson RJ. A method of analysis of back shape in scoliosis. J Biomech 1988;21:497–509.

[28] Liu XC, Thometz JG, Lyon RM, Klein J. Functional classification of patients with idiopathic scoliosis assessed by the Quantec system. Spine 2001;26:1274–9.

[29] Ajemba PO. Structured splines models: theory and application to the clinical management of torso deformities [dissertation]. Edmonton, Canada: University of Alberta, 2007.

[30] Patias P, Grivas TB, Kaspiris A, et al. A review of the trunk surface metrics used as scoliosis and other deformities evaluation indices. Scoliosis 2010;29:5–12.

[31] Ajemba PO, Durdle NG, Raso VJ. Characterizing torso shape deformity in scoliosis using structured splines models. IEEE Trans Biomed Eng 2009;56:1652–62.

[32] Goldberg CJ, Grove D, Moore DP, et al. Surface topography and vectors: a new measure for the three dimensional quantification of scoliotic deformity. Stud Health Technol Inform 2006;123:449–55.

[33] Lenke LG, Betz RR, Harms J, et al. Adolescent idiopathic scoliosis: a new classification to determine extent of spinal arthrodesis. J Bone Joint Surg Am 2001;83:1169–81.

[34] Parent EC, Zhang PQ, Hill D, et al. Sensitivity-to-change of full torso surface topography measurements in adolescents with idiopathic scoliosis and a main thoracic curve. Stud Health Technol Inform 2012;176:484.

[35] Emrani M, Kirdeikis R, Igwe P, et al. Surface reconstruction of torsos with and without scoliosis. J Biomech 2009;42:2200–4.

[36] Gwet KL. Handbook of inter-rater reliability: the definitive guide to measuring the extent of agreement among multiple raters. 2nd ed. Gaithersburg, MD: Advanced Analytics LLC, 2002:11–42.

[37] King HA, Moe JH, Bradford DS, Winter RB. The selection of fusion levels in thoracic idiopathic scoliosis. J Bone Joint Surg Am 1983;65:1302–13.

Supplementary Appendix. Technical details of creating the asymmetry deviation contour map

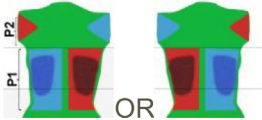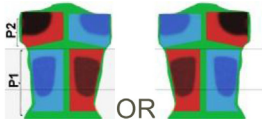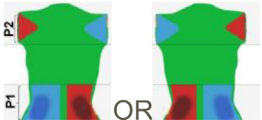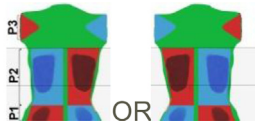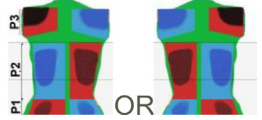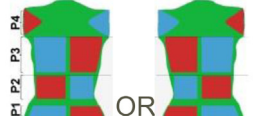### Step 1: finding the best plane of symmetry

For the first step, a subroutine was developed in Wolfram Mathematica (Mathematica, Version 8.0.4.0, Wolfram Research, Inc., Champaign, IL, USA) to find the best plane of symmetry that is approximately aligned with the midsagittal plane. The best plane of symmetry is defined as the plane that produces the minimum distance between the points of the original torso and the corresponding points of the reflected torso. For each point on the original torso, its corresponding point was the closest point on the reflected torso. The geometry of the original torso is composed of a cloud of points generated by the camera system. The software Geomagic was used to wrap a triangulated surface on the cloud of points of the original torso. The reflected torso geometry is composed of the cloud of points of the original torso after reflection (Fig. 2).

Step 2: creating the deviation contour map

For the second step, the Geomagic built-in function "3D compare" was used to draw a deviation contour map representing the distance between the points of the reflected torso and the surface of the original torso. Nine main colors were selected to simplify the display of the deviations between a minimum outward deviation of 22 mm and inward deviation of 22 mm (Fig. 3). The green color indicates a deviation of -3 to 3 mm between the original and the reflected torso. Blue colors indicate that the original torso is outside of the reflected torso and red colors indicate that the original torso is inside of the reflected torso. Light blue and yellow colors represent mild (-3 mm to -9 mm and $+3$ mm to $+9$ mm) outward and inward deviations, respectively. The dark blue and red colors indicate where the deviation is higher than the maximum and minimum deviations specified in the color mapping function (>22 mm). In other words, a dark red or dark blue color indicates a large deformation in that region (Fig. 3). Finally, the gray colors on the edges of the model show the regions where the original torso points did not have corresponding points in the reflected torso (ie, due to asymmetric cropping of the arms). The color spectrum range (± 22 mm) was chosen to provide an appropriate balance for the amount of detail shown in the asymmetry maps and was standardized for all subjects. However, for subjects with a severe torso surface deformity, a larger range for the color spectrum could be used to better visualize and locate the centers of the asymmetry regions. By virtue of the asymmetry analysis, every point in the asymmetry map with positive deviation (red color) has a corresponding point with the same magnitude but negative deviation (blue color). The color pattern is symmetric across the best plane of symmetry. A pair of corresponding blue and red colors in the asymmetry map is termed a color patch (Fig. 3).

Supplementary Table
Developed classification categories with their description

Group	Subgroup	Description of individual color patches
Group A (2 asymmetry patches)	A1 OR	First Patch: located in sections 1* and 2 with the center of deformation close to the boundary between sections 1 and 2 representing thoracic/thoracolumbar curves. Second Patch: located in section 3 and characterizes shoulder asymmetry.
	A2 OR	First Patch: same as subgroup 1. Second Patch: located in section 3 with the center of the patch located close to the scapula.
	A3 OR	First Patch: located strictly in section 1 representing lumbar curves. Second Patch: located strictly in section 3 and characterizes shoulder asymmetry.
Group B (3 asymmetry patches)	B1 OR	First Patch: located strictly in section 1 representing lumbar curves. Second Patch: located in sections 1 and 2 with the center of deformation located close to the boundary between sections 1 and 2 representing thoracic and thoracolumbar curves. Third Patch: located in section 3 and characterizes shoulder asymmetry.
	B2 OR	First and Second Patches: same as subgroup 4. Third Patch: located in section 3 with the center of the patch located close to the scapula.
Group C (4 asymmetry patches)	C1 OR	First, Second, and Third Patches: located in and between sections 1 and 2. Fourth Patch: located strictly in section 3 and characterizes shoulder asymmetry.

* Sections 1, 2, and 3 represent the bottom, middle, and top thirds of the torso, respectively.